J. Fluid Mech. (1969), *vol.* 39, *part* 3, *pp.* 587–600
Printed in Great Britain

Spherical piston problem in water

By P. L. BHATNAGAR†, P. L. SACHDEV AND PHOOLAN PRASAD

Department of Applied Mathematics, Indian Institute of Science, Bangalore 12, India

(Received 16 May 1969)

In this paper, we study the propagation of a shock wave in water, produced by the expansion of a spherical piston with a finite initial radius. The piston path in the x, t plane is a hyperbola. We have considered the following two cases: (i) the piston accelerates from a zero initial velocity and attains a finite velocity asymptotically as t tends to infinity, and (ii) the piston decelerates, starting from a finite initial velocity. Since an analytic approach to this problem is extremely difficult, we have employed the artificial viscosity method of von Neumann & Richtmyer after examining its applicability in water. For the accelerating piston case, we have studied the effect of different initial radii of the piston, different initial curvatures of the piston path in the x, t plane and the different asymptotic speeds of the piston. The decelerating case exhibits the interesting phenomenon of the formation of a cavity in water when the deceleration of the piston is sufficiently high. We have also studied the motion of the cavity boundary up to 550 cycles.

1. Introduction

In the present paper we have studied the compression waves produced in water by the non-uniform expansion of a spherical piston for different piston paths in the x, t plane both when it accelerates and when it decelerates. The problem of the uniform expansion of a sphere, with zero initial radius, in air was solved by Taylor (1946) by numerical integration of the ordinary differential equations in the similarity variable. Yeh (1962, p. 1431) extended these results for water. Naugolnykh (1966) obtained an approximate analytical solution for this problem, retaining the most dominant non-linear term. This solution for small Mach numbers is in good agreement with Taylor's solution. Lighthill (1948) has discussed this problem for a gas for both spherical and cylindrical pistons while illustrating a general method for solving a class of aerodynamic problems involving small disturbances which may include weak shocks in the flow. He has determined the order of the shock strength in terms of the Mach number of the piston and finds that the shock strength is extremely small for small piston Mach numbers, confirming earlier results of Taylor (1946). In this paper he commented that the solution of this problem, obtained by expanding the velocity potential in the powers of some small parameters, say the Mach

† Present address: University of Rajasthan, Jaipur, India.

number of the piston, exhibits certain weaknesses, namely: (i) the solution does not converge near the leading characteristic, though it gives good results elsewhere; (ii) in the expansion procedure, the disturbance is always confined within a sphere whose surface expands with the sound speed in the undisturbed medium; and (iii) across this sphere the velocity and pressure remain continuous up to the first two terms in the expansion so that there is no possibility of fitting a shock.

In a later paper, Lighthill (1949) has overcome the difficulties of the divergence of the solution near the leading characteristic by the well-known PLK method which involves the expansion of the dependent as well as the independent variables in terms of the powers of the small expansion parameter.

In the present paper we have studied this problem in water in a general way, assuming the initial radius of the piston to be finite and the piston path to be a hyperbola in the x, t plane. We consider both cases when the piston accelerates starting from zero initial velocity and when it decelerates from a finite initial velocity. Analytic approach to this problem is extremely difficult and we therefore have to employ numerical techniques to solve it. Since, for water, the energy equation is not used, we cannot use the method of artificial heat-conduction (Sachdev & Prasad 1966) evolved by us. We therefore use the method of artificial viscosity given by von Neumann & Richtmyer (1950). We examine the applicability of this method in the case of water and find that, though the thickness of the shock transition region depends on the shock strength, it lies in a small range so that this method can be successfully employed in the present case. The corresponding problem of waves produced by the non-uniform motion of a cylindrical piston has been worked out by Pandey & Prasad (1969).

2. Artificial viscosity term for water

We briefly discuss the applicability of the artificial viscosity term for water. Using the notations of von Neumann & Richtmyer and closely following their analysis, we have the following equation for the steady state solution, giving the shock transition region:

$$\left(\frac{dV}{dw}\right)^2 = \frac{\psi(\eta, \eta_f)}{(c\Delta x)^2}(V_i - V)(V - V_f), \tag{2.1}$$

which corresponds to equation (28) of von Neumann & Richtmyer. Here V is the specific volume, V_i and V_f are values of V ahead of and behind the shock respectively and w is the Lagrangian distance measured from the point where $V = \frac{1}{2}(V_i + V_f)$ and

$$\psi(\eta, \eta_f) = \frac{1}{\eta^6(1-\eta_f^7)} \sum_{i=1}^{6} \eta_f^{6-i}\eta^i(1-\eta_f^{i+1}), \tag{2.2}$$

$$\eta = \frac{V}{V_i}, \quad \eta_f = \frac{V_f}{V_i}. \tag{2.3}$$

In establishing (2.1) we have used the equation of state for water, giving the pressure

$$p = AV^{-\gamma} - B \quad \text{with} \quad \gamma = 7 \tag{2.4}$$

instead of the energy equation (18) of von Neumann & Richtmyer. We can now show that, for

$$0 < \eta_f \leqslant \eta \leqslant 1, \tag{2.5}$$

$$1 < \psi(\eta, \eta_f) < 7. \tag{2.6}$$

If the values $V = V_i$ and $V = V_f$ are attained at $w = w_i$ and $w = -w_f$ respectively, we can show that

$$w_i = \int_0^1 \frac{c\Delta x\, d\phi}{[\psi(\eta, \eta_f)(1-\phi^2)]^{\frac{1}{2}}} \tag{2.7}$$

and

$$w_f = -\int_0^{-1} \frac{c\Delta x\, d\phi}{[\psi(\eta, \eta_f)(1-\phi^2)]^{\frac{1}{2}}} \tag{2.8}$$

where

$$\phi = \frac{V - \frac{1}{2}(V_i + V_f)}{\frac{1}{2}(V_i - V_f)}$$

and the width of the shock $w_i + w_f$ satisfies the inequalities

$$\frac{1}{\sqrt{7}} < \frac{w_i + w_f}{\pi c \Delta x} < 1. \tag{2.9}$$

Thus the shock thickness, though a function of the shock strength, lies in a fairly small interval and does not present any difficulty in numerical work. In dealing with problems for water, V remains close to unity and actual variation of $w_i + w_f$ with shock strength is very small.

Though in the above analysis we have taken only one integral value of $\gamma (= 7)$, we surmise that, even for other values of γ, the artificial viscosity term is adequate.

The system of difference equations for water is the same as in von Neumann & Richtmyer except that the energy equation (51) of their paper is replaced by

$$p_{l+\frac{1}{2}}^{n+1} = \frac{A}{(V_{l+\frac{1}{2}}^{n+1})^{\gamma}} - B. \tag{2.10}$$

The stability conditions for this system of difference equations for rapidly varying perturbations are found to be

$$\frac{\Delta t}{\Delta x} \leqslant \left[\frac{V\rho_0^2}{\gamma(p+B)}\right]^{\frac{1}{2}}, \tag{2.11}$$

in the normal region and

$$\frac{\Delta t}{\Delta x} < \frac{1}{2c}\left[\frac{\rho_0^2 V_f}{(p_f+B)\{7(1-\eta_f) - \eta_f(1-\eta_f^7)\}}\right]^{\frac{1}{2}}, \tag{2.12}$$

in the shock region.

3. Piston problem with variable speed of the piston

We consider the motion produced by a spherical piston of initial radius X_0', the undisturbed water being at a constant pressure p_0 and specific volume V_0. We assume the piston path to be the hyperbola

$$X = X_0' + m_2 t + \delta \frac{m_1}{m}\{(1 + m^2 t^2)^{\frac{1}{2}} - 1\}, \tag{3.1}$$

where m_2 is the initial piston velocity, $m_2+\delta m_1$ is its final velocity and δ is $+1$ or -1 according as the piston accelerates or decelerates. The piston takes $1/m\sqrt{3}$ units of time to attain the mean of initial and final asymptotic speed.

On reducing the equation of motion to non-dimensional form with the help of the variables p_0, ρ_0, c_0 (sound speed) and a characteristic length given by the distance travelled by the sound wave in the undisturbed state in a unit time, we obtain

$$\frac{\partial U}{\partial t} = -\frac{1}{\gamma(1+\bar{B})}\left(\frac{X}{x}\right)^2 \frac{\partial}{\partial x}(p+q), \tag{3.2}$$

$$\frac{\partial X}{\partial t} = U, \tag{3.3}$$

$$\frac{\partial V}{\partial t} = \left(\frac{X}{x}\right)^2 \frac{\partial U}{\partial x} + \frac{2UV}{X}, \tag{3.4}$$

$$q = -\frac{(c\Delta x)^2}{2V}\gamma(1+\bar{B})\frac{\partial U}{\partial x}\left\{\left|\frac{\partial U}{\partial x}\right| - \frac{\partial U}{\partial x}\right\}. \tag{3.5}$$

The equation of state and the velocity of the piston in the non-dimensional form are given respectively by

$$p = \frac{\bar{A}}{V^\gamma} - \bar{B} \tag{3.6}$$

and

$$U_p = \overline{m}_2 + \delta\frac{\overline{m}_1 \overline{m}t}{\sqrt{(1+\overline{m}^2t^2)}}. \tag{3.7}$$

In equations (3.2)–(3.7), for convenience of writing, we have dropped the bars from the flow variables, but the non-dimensional parameters have bars.

The difference equations corresponding to (3.2)–(3.6) and to the boundary conditions are:

$$\frac{U_l^{n+\frac{1}{2}} - U_l^{n-\frac{1}{2}}}{\Delta t} = -\frac{1}{\gamma(1+\bar{B})}\left(\frac{X_l^n}{\bar{X}_0' + l\Delta x}\right)^2 \frac{p_{l+\frac{1}{2}}^n + q_{l+\frac{1}{2}}^{n-\frac{1}{2}} - p_{l-\frac{1}{2}}^n - q_{l-\frac{1}{2}}^{n-\frac{1}{2}}}{\Delta x}, \tag{3.8}$$

$$\frac{X_l^{n+1} + X_l^n}{\Delta t} = U_l^{n+\frac{1}{2}}, \tag{3.9}$$

$$\frac{V_{l+\frac{1}{2}}^{n+1} - V_{l+\frac{1}{2}}^n}{\Delta t} = \frac{(X_{l+1}^{n+1} + X_{l+1}^n + X_l^{n+1} + X_l^n)^2}{16[\bar{X}_0' + (l+\frac{1}{2})\Delta x]^2}\frac{U_{l+1}^{n+\frac{1}{2}} - U_l^{n+\frac{1}{2}}}{\Delta x} + 2\frac{(U_{l+1}^{n+\frac{1}{2}} + U_l^{n+\frac{1}{2}})(V_{l+\frac{1}{2}}^{n+1} + V_{l+\frac{1}{2}}^n)}{X_{l+1}^{n+1} + X_{l+1}^n + X_l^{n+1} + X_l^n}, \tag{3.10}$$

$$q_{l+\frac{1}{2}}^{n+\frac{1}{2}} = -\frac{c^2\gamma(1+\bar{B})}{V_{l+\frac{1}{2}}^n + V_{l+\frac{1}{2}}^{n+1}}(U_{l+1}^{n+\frac{1}{2}} - U_l^{n+\frac{1}{2}})[|U_{l+1}^{n+\frac{1}{2}} - U_l^{n+\frac{1}{2}}| - (U_{l+1}^{n+\frac{1}{2}} - U_l^{n+\frac{1}{2}})], \tag{3.11}$$

$$p_{l+\frac{1}{2}}^{n+1} = \frac{\bar{A}}{(V_{l+\frac{1}{2}}^{n+1})^\gamma} - \bar{B}, \tag{3.12}$$

$$\left.\begin{aligned} X_0^n &= \bar{X}_0' + \overline{m}_2(n\Delta t) + \delta\frac{\overline{m}_1}{\overline{m}}[\{1+\overline{m}^2(n\Delta t)^2\}^{\frac{1}{2}} - 1] \\ U_0^{n+\frac{1}{2}} &= \overline{m}_2 + \delta\frac{\overline{m}_1\overline{m}(n+\frac{1}{2})\Delta t}{[1+\overline{m}^2\{(n+\frac{1}{2})\Delta t\}^2]^{\frac{1}{2}}} \end{aligned}\right\} \quad \text{for} \quad n \geqslant 1. \tag{3.13}$$

We have considered two different situations regarding the initial piston speed. In the first instance, the piston starts from zero initial velocity and accelerates ($\overline{m}_2 = 0$, $\delta = 1$) so that we have the following initial conditions:

$$U_l^{-\frac{1}{2}} = 0, \quad q_{l+\frac{1}{2}}^{-\frac{1}{2}} = 0, \quad X_l^0 = X_l^{-\frac{1}{2}} = \overline{X}_0' + l\Delta x, \quad p_{l+\frac{1}{2}}^0 = V_{l+\frac{1}{2}}^0 = 1 \quad (3.14)$$

for all l.

In the second case, the piston starts with a finite initial speed $\overline{m}_2$ and decelerates according to (3.1) with $\delta = -1$. To start the solution we obtained the initial distribution of flow variables by solving the steady-state equation (2.1) with the shock located at $x = 2\Delta x$, i.e. with the condition that the non-dimensional specific volume $V = \frac{1}{2}(1+\eta_f)$ at $x = 2\Delta x$. We obtain the value of η_f from the Rankine–Hugoniot conditions, taking the particle velocity behind the shock to be $\overline{m}_2$. The error in obtaining the initial distribution of flow variables from a one-dimensional uniform solution for our spherical piston case is likely to be very small. We also calculate the time which the shock takes to propagate from the piston position $x = 0$ to $x = 2\Delta x$ for $\overline{m}_2 = 1$; we find this to be equal to $7{\cdot}04 \times 10^{-6}$. We assume the shock to move with uniform velocity during this interval.

4. Numerical results and discussions

We have carried out our computations with the following values of the constants and mesh size:

$$c = 2, \quad \gamma = 7, \quad B = 3000, \quad A = 3001, \quad x = 0{\cdot}00001.$$

The various cases considered are given in table 1.

Cases	$\overline{m}_2$	X_0'	$\overline{m}_1$	δ	$\overline{m}$	$\Delta t/\Delta x$	Initial curvature of piston path	Total time up to which result is obtained
I	0	0·01	0·23601	1	10,000	0·5	2,360·1	0·0003
II	0	0·0001	0·97212	1	30,000	0·15	29,164	0·00011
III	0	0·001	0·97212	1	30,000	0·2	29,164	0·0001
IV	0	0·001	0·97212	1	15,000	0·15	14,582	0·0002
V	0	0·0001	1·63175	1	30,000	0·05	48,952	0·0001
VI	1	0·001	0·23601	−1	30,000	0·10	25,033	0·00026
VII	1	0·001	0·60000	−1	30,000	0·10	6,364	0·00016
VIII	1	0·001	1·00000	−1	30,000	0·10	10,607	0·00055

TABLE 1

In terms of the non-dimensional variables the initial curvature of the piston path in the x, t plane is

$$\frac{\overline{m}_1 \overline{m} \delta}{(1+\overline{m}_2^2)^{\frac{3}{2}}}.$$

Table 1 shows that the initial curvature of the piston path is smallest in case I and largest in case V. The final asymptotic speed of the piston is $m_2 + m_1\delta$

so that after a long time the solution, in cases I to V, will tend to Taylor's (1946) solution when $\bar{X}_0'$ is much smaller than the distance traversed by the shock.

Figures 1–3 give pressure, velocity and specific volume distribution *versus* Lagrangian distance after a different number of cycles for case I. The choice of our scale for pressure gives an illusion that the pressure curves end on $p = 0$; in fact they end on the line $p = 1$. In this case, the initial piston radius, $\bar{X}_0'$, is very much greater than the total distance travelled by the shock or the piston so that the motion is approximately one-dimensional. The figures clearly show that the wave front is a shock which grows in strength as the speed of the piston

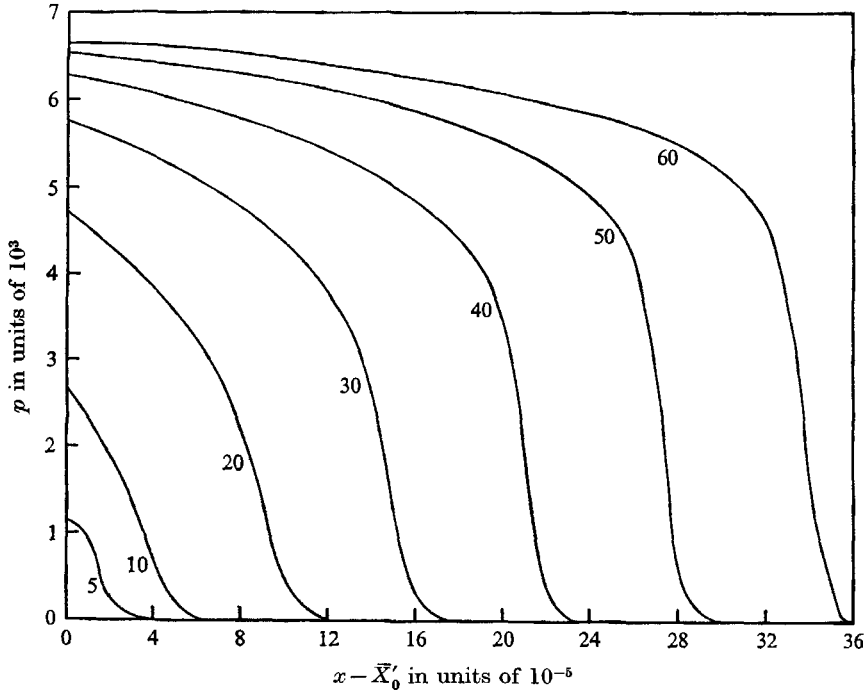

FIGURE 1. Pressure *versus* Lagrangian distance at various cycles (case I).

increases. At any fixed time, pressure, density and velocity have the greatest value at the piston and gradually decrease towards the shock. The final piston speed is subsonic with respect to undisturbed sound speed ($\bar{m}_1 = 0{\cdot}23601$). In cases II, III and IV, the final piston speed is almost sonic while it is supersonic for case V as shown in the table.

The initial radius of the piston is 0·0001 for case II and it is 0·001 for case III. After 30 cycles in case III and 40 cycles in case II (which give the same total time of the piston motion), we find from figure 4 that though the piston speed is the same in both cases the pressure rise across the shock and pressure in the region behind the shock is everywhere much smaller in case II than in case III. This clearly brings out the damping effect of the sphericity. The pressure at

the piston after 40 cycles for case II shows decrease with time and it is surmised that, after sufficiently large time, it will tend to that predicted by Yeh (1962), though we could not obtain the solution for larger time, because of the limitations of the computer.

Now we consider the effect of the initial curvature of the piston path, given by different values of $\overline{m}$ for the same value of $\overline{m}_1$. The initial curvature is larger

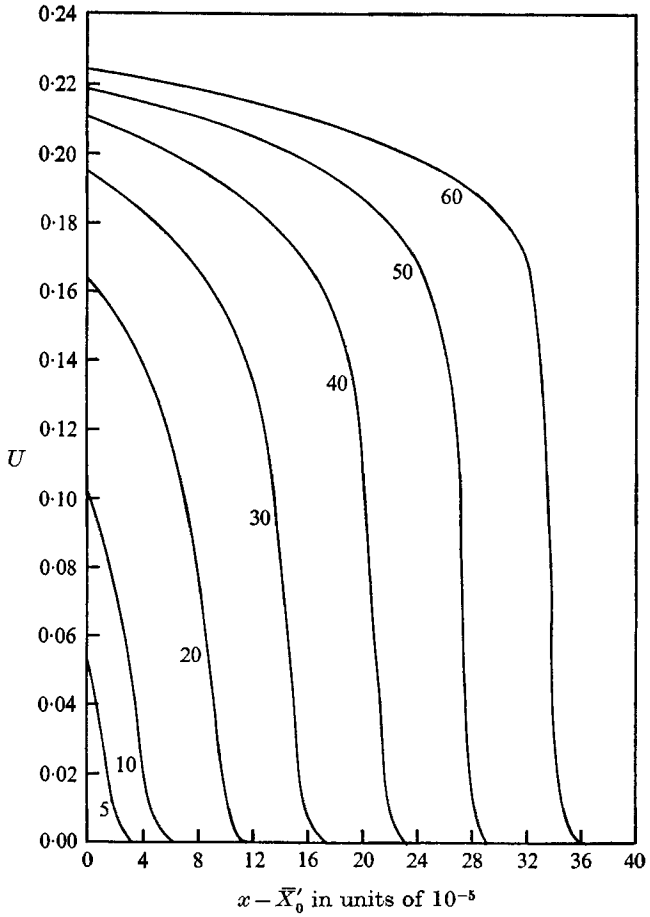

FIGURE 2. Velocity *versus* Lagrangian distance at various cycles (case I).

in case III than that in case IV. The curves in figure 5, giving the pressure distribution after 30 cycles for case III and after 40 cycles for case IV (which correspond to the same total time of the piston motion) show that the shock is stronger in case III than that in case IV. Similarly, when the piston velocity is the same for case III and case IV after 40 cycles and 110 cycles respectively, the shock is stronger in case III than that in case IV. Of course, the disturbance has traversed a much larger distance in case IV.

In case V where the piston motion is supersonic ($\overline{m}_1 > 1$), the computer was run for 200 cycles and the distribution of the flow variables is shown in

figures 6 and 7. We find that the radius of the piston (Eulerian distance) is 1·576 and 2·176 times its initial radius after 120 cycles and 200 cycles respectively (figure 7). At a given time, the specific volume is almost constant, the variation of pressure is small and the velocity varies rapidly with Lagrangian distance in the region behind the shock.

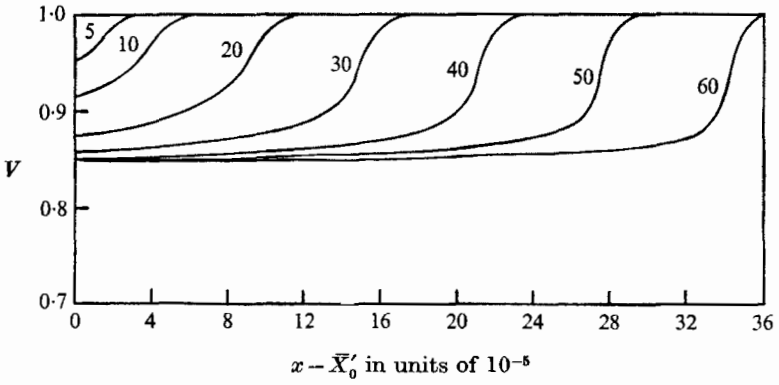

FIGURE 3. Specific volume *versus* Lagrangian distance at various cycles (case I).

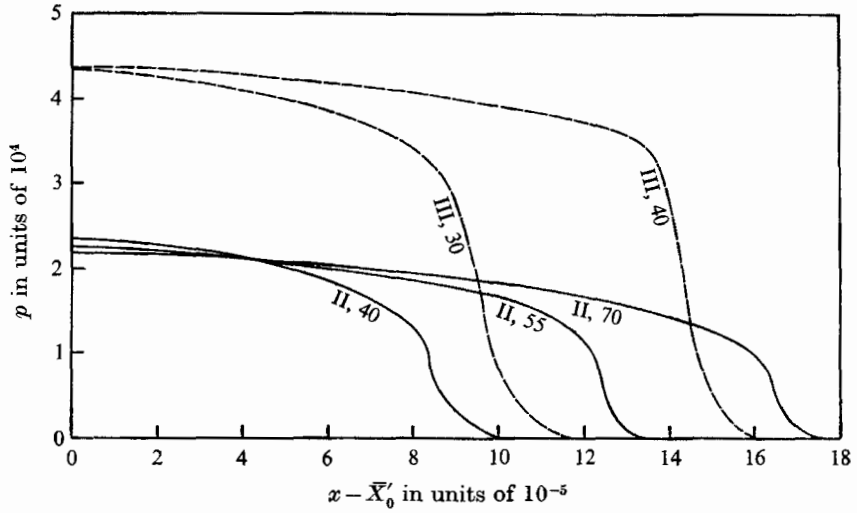

FIGURE 4. Pressure *versus* Lagrangian distance showing the effect of the initial position of the piston $\bar{X}_0'$ (cases II and III).

In cases VI, VII and VIII, the piston starts with a sonic velocity ($\bar{m}_2 = 1$) so that in the beginning a strong shock wave of Mach number 2·8397 is produced. The deceleration of the piston starts after time $7{\cdot}04 \times 10^{-6}$ and the variation of pressure, particle velocity and Eulerian position of the fluid particles have been shown graphically in figures 7 to 9 at various cycles. The dotted curves ($n = 0$) in figures 8 and 9 give the initial distributions of pressure and velocity and are common for all three cases VI, VII and VIII. The shock strength decays owing

to the deceleration of the piston and this decay is very pronounced and rapid in case VIII. In case VI, the pressure is almost constant from the piston to the shock at the 260th cycle but the velocity monotonically decreases. In case

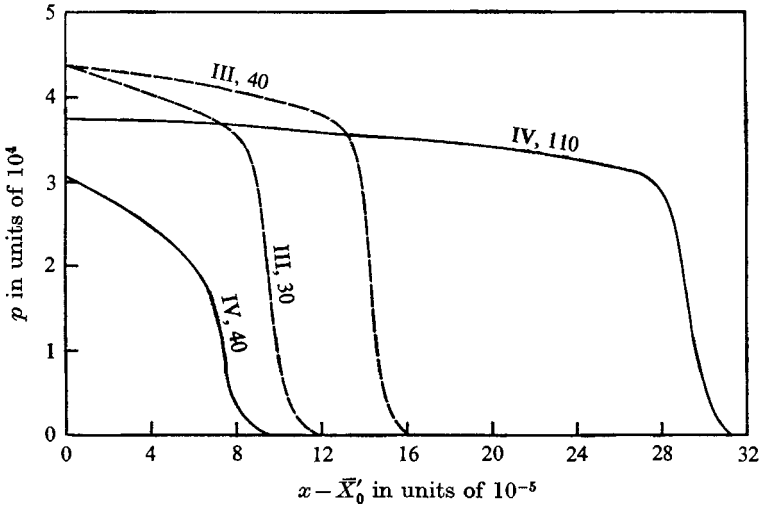

FIGURE 5. Pressure *versus* Lagrangian distance showing the effect of the curvature of the piston path in x, t plane (cases III and IV).

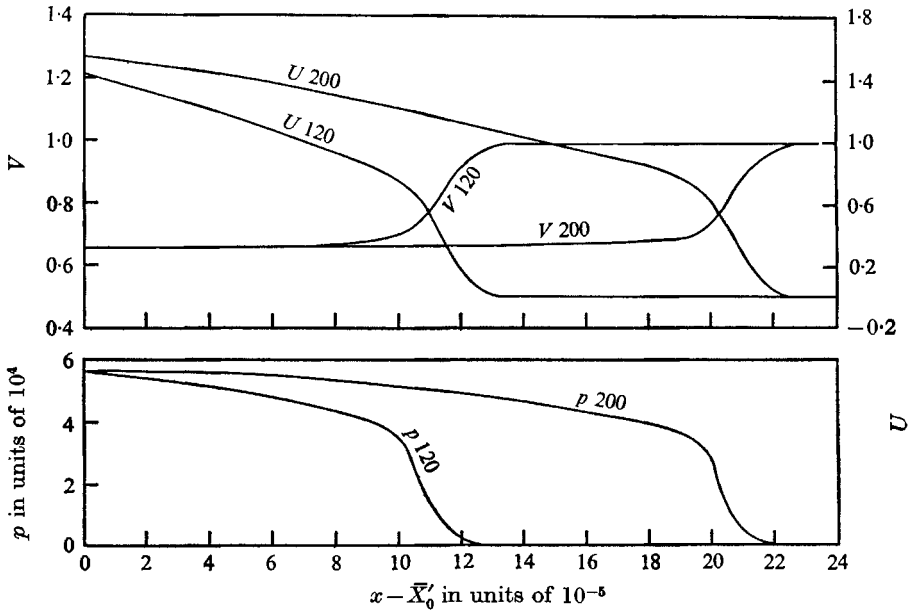

FIGURE 6. Velocity, pressure and specific volume *versus* Lagrangian distance at various cycles (case V).

VIII, the piston comes to rest as t tends to infinity and the deceleration is so large that pressure becomes zero at the piston when $n = 70$ and after that a cavity is formed between the piston and the water.

The particle velocity monotonically increases from the piston to the shock for case VIII. As we go from case VIII to case VI through case VII, the deceleration of the piston decreases and the variation of velocity from piston to shock is less pronounced and for the same case, say VI, the approach of the

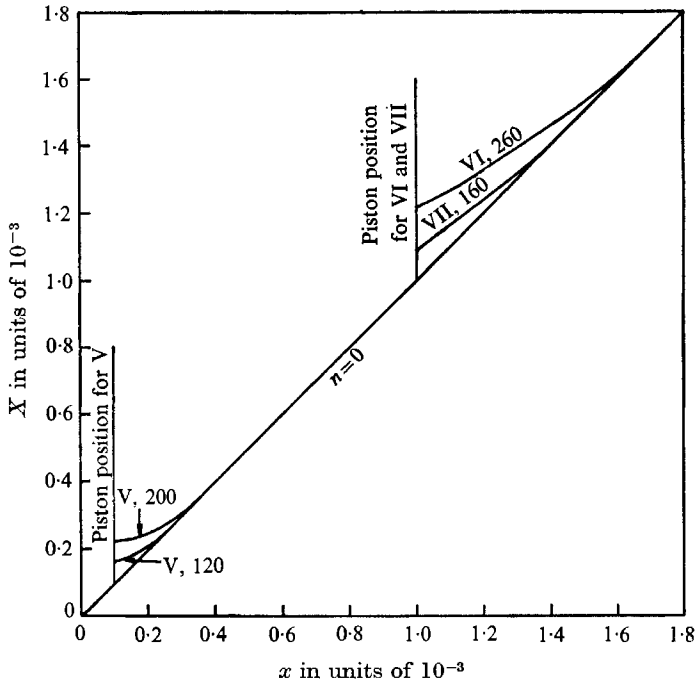

FIGURE 7. Eulerian distance *versus* Lagrangian distance (cases V, VI and VII).

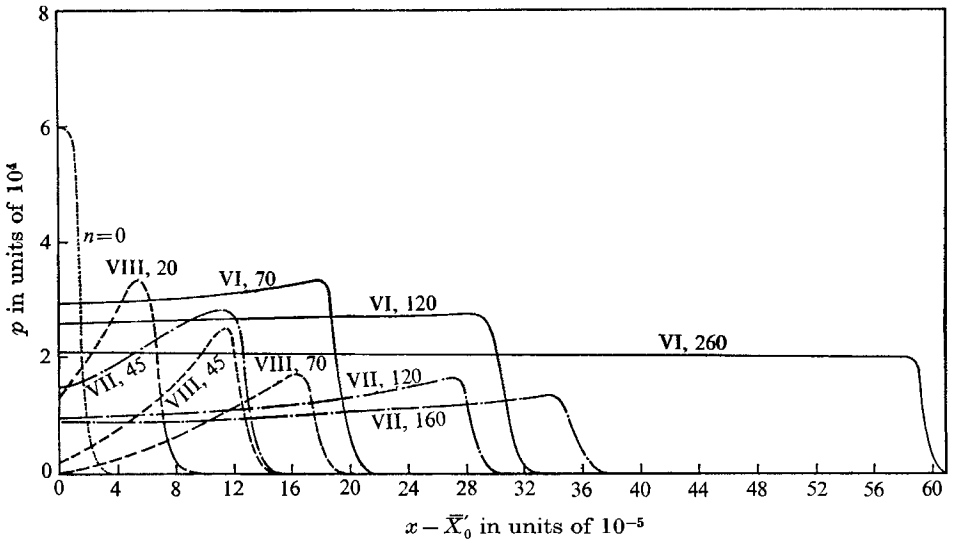

FIGURE 8. Pressure *versus* Lagrangian distance showing the effect of deceleration of the piston (cases VI, VII and VIII).

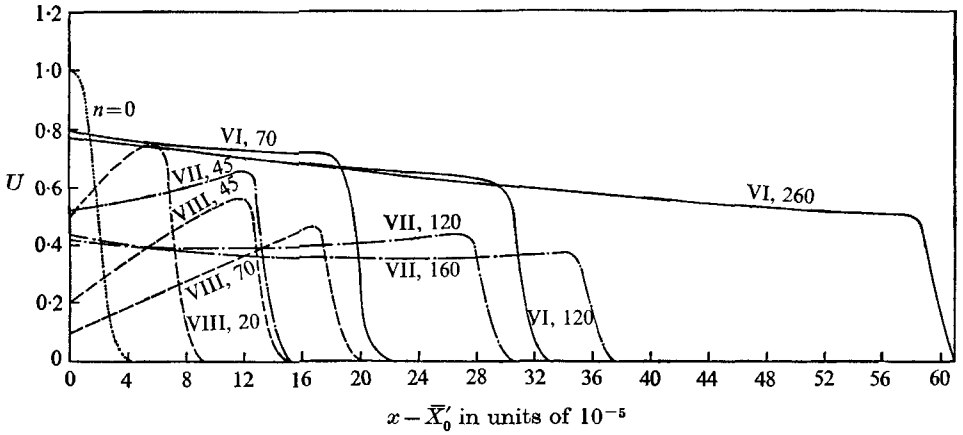

FIGURE 9. Particle velocity *versus* Lagrangian distance showing the effect of deceleration of the piston (cases VI, VII and VIII).

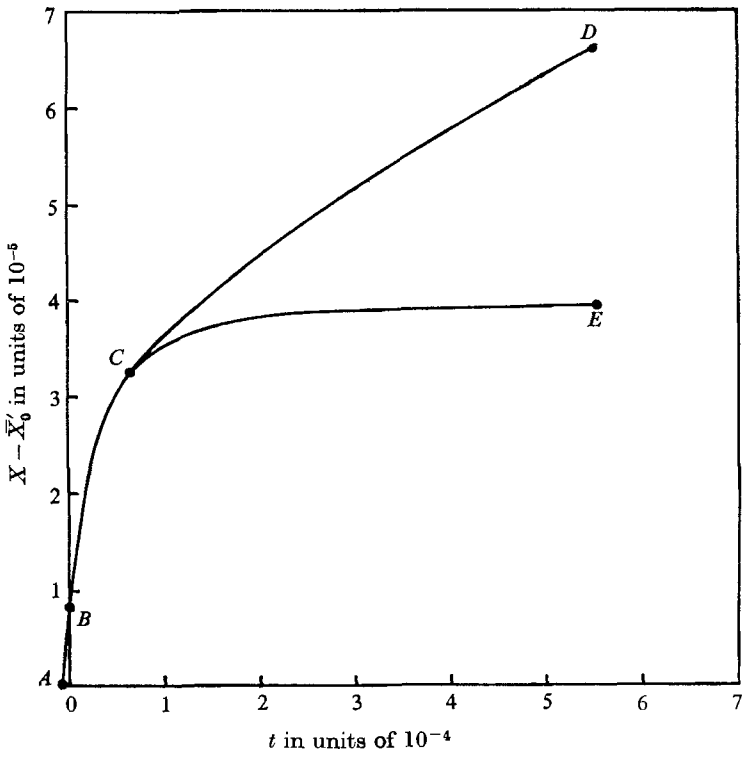

FIGURE 10. Piston and cavity paths in X, t plane. $ABCE$, piston path; CD, cavity path.

particle velocity to the limiting velocity distribution as t tends to infinity is more rapid than the approach of the pressure to the limiting pressure distribution. To study the approach of pressure to the limiting pressure distribution in each case, integration over a larger number of cycles is needed, but this study does not seem to yield any significant information so we did not undertake further computation.

Motion of the cavity

Figures 10 and 11 show the piston and cavity paths in the x, t plane and the distribution of velocity behind the shock at different cycles respectively for the case VIII of a decelerating piston in which a cavity is formed at $n = 70$.

l	X_l^n	$U_l^{n-\frac{1}{2}}$	$l+\frac{1}{2}$	$V_{l+\frac{1}{2}}^n$	$p_{l+\frac{1}{2}}^n$
0	$1{\cdot}03301 \times 10^{-3}$	$1{\cdot}08202 \times 10^{-1}$	0·5	1·000050	0
1	$1{\cdot}04250 \times 10^{-3}$	$1{\cdot}18022 \times 10^{-1}$	1·5	0·975765	$5{\cdot}63283 \times 10^{2}$
2	$1{\cdot}05173 \times 10^{-3}$	$1{\cdot}40707 \times 10^{-1}$	2·5	0·951479	$1{\cdot}25080 \times 10^{3}$
3	$1{\cdot}06067 \times 10^{-3}$	$1{\cdot}64353 \times 10^{-1}$	3·5	0·929149	$2{\cdot}01961 \times 10^{3}$
4	$1{\cdot}06940 \times 10^{-3}$	$1{\cdot}88968 \times 10^{-1}$	4·5	0·907999	$2{\cdot}89840 \times 10^{3}$
5	$1{\cdot}07800 \times 10^{-3}$	$2{\cdot}14982 \times 10^{-1}$	5·5	0·888035	$3{\cdot}89057 \times 10^{3}$
6	$1{\cdot}08644 \times 10^{-3}$	$2{\cdot}40001 \times 10^{-1}$	6·5	0·871849	$4{\cdot}83750 \times 10^{3}$
7	$1{\cdot}09476 \times 10^{-3}$	$2{\cdot}57700 \times 10^{-1}$	7·5	0·860790	$5{\cdot}57011 \times 10^{3}$
8	$1{\cdot}10300 \times 10^{-3}$	$2{\cdot}77029 \times 10^{-1}$	8·5	0·843086	$6{\cdot}91204 \times 10^{3}$
9	$1{\cdot}11109 \times 10^{-3}$	$3{\cdot}24139 \times 10^{-1}$	9·5	0·818369	$9{\cdot}20733 \times 10^{3}$
10	$1{\cdot}11899 \times 10^{-3}$	$3{\cdot}38590 \times 10^{-1}$	10·5	0·824086	$8{\cdot}72673 \times 10^{3}$
11	$1{\cdot}12697 \times 10^{-3}$	$3{\cdot}16249 \times 10^{-1}$	11·5	0·816313	$9{\cdot}42420 \times 10^{3}$
12	$1{\cdot}13490 \times 10^{-3}$	$3{\cdot}86947 \times 10^{-1}$	12·5	0·787155	$1{\cdot}30267 \times 10^{4}$
13	$1{\cdot}14258 \times 10^{-3}$	$3{\cdot}85529 \times 10^{-1}$	13·5	0·794348	$1{\cdot}20380 \times 10^{4}$
14	$1{\cdot}15037 \times 10^{-3}$	$4{\cdot}18121 \times 10^{-1}$	14·5	0·768288	$1{\cdot}59932 \times 10^{4}$
15	$1{\cdot}15793 \times 10^{-3}$	$4{\cdot}31711 \times 10^{-1}$	15·5	0·778159	$1{\cdot}43695 \times 10^{4}$
16	$1{\cdot}16562 \times 10^{-3}$	$4{\cdot}42407 \times 10^{-1}$	16·5	0·755397	$1{\cdot}83815 \times 10^{4}$
17	$1{\cdot}17312 \times 10^{-3}$	$4{\cdot}58810 \times 10^{-1}$	17·5	0·796471	$1{\cdot}17597 \times 10^{4}$
18	$1{\cdot}18105 \times 10^{-3}$	$2{\cdot}65212 \times 10^{-1}$	18·5	0·909804	$2{\cdot}81608 \times 10^{3}$
19	$1{\cdot}19014 \times 10^{-3}$	$6{\cdot}04749 \times 10^{-2}$	19·5	0·986179	$3{\cdot}08070 \times 10^{2}$
20	$1{\cdot}20000 \times 10^{-3}$	$2{\cdot}48106 \times 10^{-3}$	20·5	0·999567	$1{\cdot}01210 \times 10$
21	$1{\cdot}21000 \times 10^{-3}$	$3{\cdot}32335 \times 10^{-5}$	21·5	0·999994	1·11592

TABLE 2. Distribution of flow variables (case VIII) when a cavity appears at $n = 70$ in the flow

We have followed the motion of the cavity by imposing the boundary condition that the pressure at the cavity is zero and therefore the specific volume at the cavity is $(\bar{A}/\bar{B})^{1/\gamma}$. This gives us the boundary conditions

$$p_{\frac{1}{2}}^{n+1} = 0, \quad V_{\frac{1}{2}}^{n+1} = \left(\frac{\bar{A}}{\bar{B}}\right)^{1/\gamma}, \tag{4.1}$$

instead of conditions (3.13) at the piston. Equations (3.9) and (3.10) are iteratively solved for cavity position X_0^{n+1} and cavity velocity $U_0^{n+\frac{1}{2}}$ satisfying the above boundary conditions. We have neglected the small vapour pressure within the cavity.

Figure 10 shows that the piston gets detached from the fluid at $n = 70$ and

then decelerates to rest while the cavity wall moves away from the piston. Up to $n = 550$ the cavity continues to move away from the piston and we presume that finally it comes to rest and moves back to collide with the piston. However, we have not carried out integrations for this phase of cavity motion. Table 2 gives the distribution of flow and physical variables behind the shock at

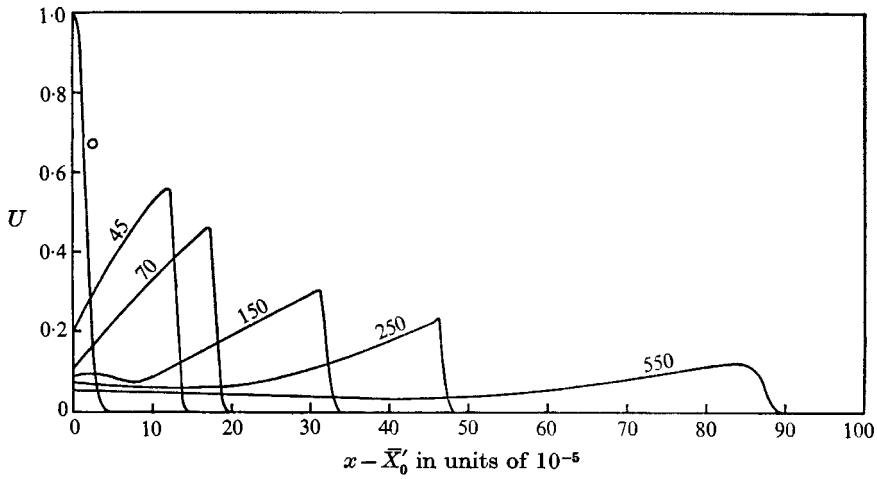

FIGURE 11. Particle velocity *versus* Lagrangian distance for case VIII (with a cavity after $n = 70$).

$l+\frac{1}{2}$	$n = 70$	$n = 150$	$n = 350$	$n = 550$
0·5	0	0	0	0
5·5	3,891	231	55	23
10·5	8,626	710	106	43
15·5	14,370	2,424	168	65
19·5	28,161†	...	...	...
20·5	10	4,421	220	87
25·5	1	7,437	333	113
30·5	1	10,558†	385	150
35·5	1	1	896	167
40·5	1	1	1,558	210
45·5	1	1	2,051	268
50·5	1	1	3,182	325
55·5	1	1	3,574	520
59·5	1	1	5,311†	...
60·5	1	1	4,245	886
65·5	1	1	1	1,215
70·5	1	1	1	1,496
75·5	1	1	1	2,304
80·5	1	1	1	2,530
85·5	1	1	1	3,573†
90·5	1	1	1	4
95·5	1	1	1	1

† Represents the position of the shock.

TABLE 3. Distribution of pressure (case VIII) at various cycles

the instant of cavity formation, i.e. when $n = 70$. Table 3 shows the distribution of pressure behind the shock at $n = 70$, 150, 350, 550. We find that the pressure in the fluid in the neighbourhood of the cavity is of the order of a few atmospheres while it is zero at the boundary of the cavity. Figure 11 shows that the velocity is no longer monotonic but has a minimum value between the cavity wall and the shock.

The authors express their thanks to Mr S. S. Krishna Murthy who carried out the complicated programming of this problem on the CDC 3600 computer at TIFR, Bombay.

REFERENCES

LIGHTHILL, M. J. 1948 *Quart. J. Mech. Appl. Math.* **1**, 309.

LIGHTHILL, M. J. 1949 *Phil. Mag.* **40**, 1179.

NAUGOLNYKH, K. A. 1966 *Soviet Phys. Acoustics*, **11**, 296.

PANDEY, B. C. & PRASAD, P. 1969 To be published. *Defence Sci. J. India.*

SACHDEV, P. L. & PRASAD, P. 1966 *J. Phys. Soc. Japan*, **21**, 2715.

TAYLOR, G. I. 1946 *Proc. Roy. Soc. Lond.* A **186**, 273.

VON NEUMANN, J. & RICHTMYER, R. D. 1950 *J. Appl. Phys.* **21**, 232.

YEH, G. C. K. 1962 *Proc. Fourth U.S. National Congress Applied Mechanics.* California University, Vol. II, 1431.